The Journal of Nutrition
Nutrient Physiology, Metabolism, and Nutrient-Nutrient Interactions

Dietary Quercetin Reduces Plasma and Tissue Methylglyoxal and Advanced Glycation End Products in Healthy Mice Treated with Methylglyoxal

Yantao Zhao, Yao Tang, and Shengmin Sang

Laboratory for Functional Foods and Human Health, Center for Excellence in Post-Harvest Technologies, North Carolina Agricultural and Technical State University, North Carolina Research Campus, Kannapolis, NC, USA

ABSTRACT

Background: Methylglyoxal (MGO), a precursor of advanced glycation end products (AGEs), has been linked to AGEs-associated diseases.

Objectives: This study investigated the efficacy and mechanisms of dietary quercetin in decreasing plasma and tissue concentrations of MGO and AGEs in MGO-administered mice.

Methods: Male, 6-wk-old CD-1 mice were administered AIN-93G diet and water (Con) or 0.12% MGO in water (MGO) or MGO plus 0.2% (0.2Q) dietary quercetin for 1 wk ($n = 5$) (experiment 1), and water (Con), 0.12% MGO (MGO), or MGO plus 0.1% (0.1Q), 0.2% (0.2Q), or 0.4% (0.4Q) dietary quercetin for 6 wk ($n = 10$) (experiment 2). The plasma, kidney, and liver concentrations of MGO, quercetin, and isorhamnetin and their trapping adducts with MGO were determined by LC-MS, and AGE concentrations were measured by the fluorescent method. Furthermore, the expressions of glyoxalase I/II (GLO I/II) and aldose reductase (AR), MGO detoxification enzymes, were determined by Western blot. One-factor ANOVA and post hoc Dunnett's or Tukey's test were used to analyze the data.

Results: After 1 wk of treatment, the MGO concentrations in plasma (20.2%) and kidney (29.9%) in 0.2Q mice were significantly lower than those in MGO mice. After 6 wk of treatment, the concentrations of MGO in the plasma (14.7–18.6%), kidney (20–20.8%), liver (15.4–18.6%), and tissue AGEs (28–36.8%) in 0.1Q, 0.2Q, and 0.4Q mice were significantly lower than those in MGO mice. The plasma concentrations of quercetin, isorhamnetin, and their MGO adducts were dose-dependently increased after quercetin administration. In addition, after 6 wk of quercetin administration, the expressions of GLO I/II and AR in the liver and kidney were significantly upregulated to promote MGO detoxification compared with MGO-treated mice.

Conclusions: Quercetin reduced plasma and tissue MGO concentrations and inhibited AGE formation by trapping MGO and regulating the MGO detoxification systems in MGO-administered healthy mice. *J Nutr* 2021;151:2601–2609.

Keywords: methylglyoxal, advanced glycation end products, quercetin, direct trapping, detoxification pathway

Introduction

Advanced glycation end products (AGEs) are complex, stable, irreversible, and nondigestible compounds that are formed exogenously during food preparation through Maillard reactions and endogenously involving glucose, protein, lipid, and nucleic acid, respectively (1, 2). Increasing evidence has identified the formation and accumulation of AGEs involved in the pathogenesis of numerous chronic diseases, such as diabetes and its complications, atherosclerosis, obesity, renal failure, aging, and Alzheimer disease (2–8).

Methylglyoxal (MGO), also known as 2-oxopropanal or pyruvaldehyde, is a reactive intermediate of several metabolic pathways and is inevitably produced in the course of metabolism, even under normal physiological conditions (9). MGO is 1 of the highly reactive dicarbonyl species, which are precursors of AGE formation and triggers of oxidative stress (9–11). MGO contributes to the formation of irreversible AGEs by binding to and modifying arginine, lysine, and cysteine residues in organisms. Many MGO-derived AGEs, such as arginine-derived hydroimidazolone N-(5-hydro-5-methyl-4-imidazolon-2-yl)-ornithine (MG-H1), N-carboxyethyl-lysine (CEL), argpyrimidine, lysine-derived 4-methylimidazolium crosslink (MOLD), and the arginine-lysine-derived crosslink 2-ammonio-6-([2-[(4-ammonio-5-oxido-5-oxopentyl)amino]-4-methyl-4,5-dihydro-1H-imidazol-5-ylidene]amino) hexanoate (MODIC) have been identified and used as biomarkers of AGEs (12, 13).

Manuscript received January 22, 2021. Initial review completed March 15, 2021. Revision accepted May 11, 2021.
First published online June 5, 2021; doi: https://doi.org/10.1093/jn/nxab176.

In addition to the endogenous MGO in the body, MGO is also present in many food products, like carbonated soft drinks, honey, cookies, cheese, and bread (14, 15). Exogenous MGO administration in animals has been used to establish the models of type 2 diabetes and its complications and also, together with a high-fat diet, to induce metabolic syndrome in mice (16–21).

Quercetin, a flavonoid widely found in many fruits, vegetables, leaves, and grains, and a popular commercial supplement, has positive antiglycation effects through trapping MGO under in vitro conditions (22–24). A recent human study reported that a 4-wk treatment of quercetin 3-glucoside at a dose of 160 mg/d decreased plasma MGO concentrations in apparently healthy (pre)hypertensive adults (25). However, the exact mechanisms and the dose effects of quercetin in lowering MGO and AGEs concentrations in vivo remain unclear. Therefore, in the present study, mice administered exogenous MGO were used to investigate whether dietary quercetin could dose-dependently reduce the concentrations of MGO and AGEs through trapping MGO and activating MGO detoxification pathways.

Material and Methods

Chemicals and reagents

Quercetin, isorhamnetin, methylglyoxal solution (40% in water), 2,4-dinitrophenylhydrazine (DNPH), and other chemicals were purchased from Sigma. The primary antibodies against glyoxalase I and II (GLO I and II; sc-67351 and sc-51091), and aldose reductase (AR; sc-166918), β-actin (#4970), and horseradish peroxidase (HRP)–conjugated anti–rabbit, –mouse, and –goat IgG were purchased from Santa Cruz Biotechnology, Cell Signaling, and Thermo Fisher Scientific, respectively. HPLC and LC-MS–grade solvents and other reagents were obtained from VWR International and Thermo Fisher Scientific.

Animals and treatments

CD-1 mice were used in this study because they are ideal and popular in general multipurpose models for safety and efficacy testing (26). Male CD-1 mice (5 wk old) were obtained from Charles River Laboratories. All of the mice were acclimated for 1 wk before being randomly placed in different experimental groups. The experimental animal protocol was approved by the Institutional Animal Care and Use Committee of the North Carolina Research Campus (protocol 19-015).

Experiment 1

Fifteen mice were placed in 3 groups ($n = 5$ per group) and given the following treatments for 1 wk: *1*) control group (Con), given the control diet (AIN-93G) and normal drinking water; *2*) MGO group (MGO), given the AIN-93G diet and 0.12% MGO in drinking water; and *3*) 0.2% quercetin group (0.2Q), given 0.2% (wt/wt) quercetin in AIN-93G diet and 0.12% MGO in drinking water.

Experiment 2

To investigate whether the extended period of treatment and different doses of quercetin would show better efficacy, another mouse experiment with a 6-wk treatment was designed and conducted. Fifty mice were divided into 5 groups ($n = 10$ per group) and given the following treatments for 6 wk: *1*) control group (Con), *2*) MGO group (MGO), and *3*–*5*) 0.1%, 0.2%, and 0.4% quercetin groups (0.1Q, 0.2Q, and 0.4Q), respectively, given 0.1%, 0.2%, and 0.4% (wt/wt) quercetin in the AIN-93G diet and 0.12% MGO in drinking water. Based on the recommended and used doses of the commercial quercetin supplement in humans and the dosage published in the human study (27), the current equivalent doses of quercetin at 0.1%, 0.2%, and 0.4% can be achievable and safe in humans.

Body weight (BW) and food and fluid intakes were measured weekly. MGO and quercetin administration did not change the food intake. The average daily food intake for all groups was 4 g diet/mouse. Therefore, the daily quercetin intakes were 4 mg (93 mg/kg BW), 8 mg (183 mg/kg BW), and 16 mg (367 mg/kg BW) per mouse in the 0.1Q, 0.2Q, and 0.4Q groups, respectively. The average daily fluid intakes per mouse were in the range of 3.7 to 4.1 mL, which provided 4.4–5.0 mg MGO (from 101 to 114 mg/kg BW) to each mouse per day. There was a slight decrease in fluid intake in 0.2Q (by 9%) and 0.4Q (by 11%) compared with MGO. Mice were group housed (5 mice per cage, 1 cage/treatment for experiment 1, and 2 cages/treatment for experiment 2). Therefore, we were not able to conduct statistical analyses of daily food and fluid intakes.

Five mice from each group were placed into 1 metabolic cage and their pooled fecal and urine samples were obtained over a 24-h period. At the end of the treatment, the mice were killed and the blood, liver, and kidney samples were collected, frozen under liquid nitrogen, and stored at −80°C until further analyses.

Exogenous MGO administration in drinking water was used in both mouse studies to mimic the conditions of human consumption of beverages, honey, and foods with high MGO content, and high plasma MGO concentrations in diabetic patients. The power and sample size calculations were employed by G-Power software based on our previous results. In the previous study (21), the mice were treated with 0.12–0.2% MGO for 17 wk ($n = 15$), and the effect size of elevated plasma MGO concentration was 3.53 compared with the control mice. We assumed that the MGO treatment effect is time dependent and the effect size of 0.12% MGO treatment for 6 wk is 1.25 (6/17 of the effect size of the 17 wk treatment), and therefore $n = 10$ mice per treatment provide 84.9% of power to detect the effects of plasma MGO at $\alpha = 0.05$. Experiment 1 is a pilot study; therefore, we used only 5 mice per group.

Measurements of MGO in the plasma, liver, and kidney by LC-MS

The MGO concentrations in the plasma, liver, and kidney were determined using the DNPH derivatization method by LC-MS as previously described (28).

Measurements of AGEs in the kidney and liver

The AGE concentrations in the kidney and liver were determined as previously described based on the specific fluorescent characteristics of AGEs (21, 29, 30).

Determination and quantification of quercetin, isorhamnetin, and their MGO adducts in plasma, urine, feces, kidney, and liver

Preparation of plasma and urine samples.

The urine and plasma samples (200 μL) were mixed with the enzymes of glucuronidase/sulfatase (30:1, 50 μL), vitamin C (40 μL), and sodium acetate buffer (100 mM, pH 5.0, 310 μL), and then the mixture was put on a shaker at 37°C for 3 h. The hydrolysis was terminated with 2M HCl (20 μL) and centrifuged at 16,000 × g for 15 min at 4

Partially supported by funding from the USDA National Institute of Food and Agriculture (NIFA) grant 2012-38821-20012 to SS.
Author disclosures: The authors report no conflicts of interest.
Supplementary Methods and Supplemental Figure 1 are available from the "Supplementary data" link in the online posting of the article and from the same link in the online table of contents at https://academic.oup.com/jn.
Address correspondence to SS (e-mails: ssang@ncat.edu, or shengminsang@yahoo.com).
Abbreviations used: ACN, acetonitrile; AGEs, advanced glycation end products; AR, aldose reductase; AU, arbitrary units; BW, body weight; CEL, N-carboxyethyl-lysine; Con, Control mice fed AIN-93G diet and water; DNPH, 2,4-Dinitrophenylhydrazine; FA, formic acid; GLO, glyoxalase; HFD, high-fat diet; LOD, limit of detection; LOQ, limit of quantification; MG-H1, arginine-derived hydroimidazolone N-(5-hydro-5-methyl-4-imidazolon-2-yl)-ornithine; MGO, methylglyoxal or mice fed AIN-93G diet and 0.12% MGO in water; MODIC, arginine-lysine-derived crosslink 2-ammonio-6-([2-[(4-ammonio-5-oxido-5-oxopentyl)amino]-4-methyl-4,5-dihydro-1H-imidazol-5-ylidene]amino) hexanoate; MOLD, lysine-derived 4-methylimidazolium crosslink; RAGE, receptor for AGEs; 0.1Q, mice fed 0.1% quercetin in diet plus 0.12% MGO in water; 0.2Q, mice fed 0.2% quercetin in diet plus 0.12% MGO in water; 0.4Q, mice fed 0.4% quercetin in diet plus 0.12% MGO in water.

TABLE 1 Body and organ weights of mice fed the control diet and water (Con) or 0.12% MGO in water (MGO), or 0.12% MGO in water and diet containing 0.1Q, 0.2Q, or 0.4Q for 6 wk (experiment 2)[1]

	Con	MGO	0.1 Q	0.2 Q	0.4 Q
Initial BW, g	34.0 ± 3.58	36.2 ± 3.48	34.8 ± 2.41	34.1 ± 2.32	34.7 ± 1.78
Final BW, g	41.9 ± 5.32[2]	48.1 ± 5.80	43.0 ± 6.03	43.7 ± 4.80	43.5 ± 4.88
Weight gain, g/6 wk	7.90 ± 2.22[2]	11.9 ± 2.90	8.22 ± 4.18[2]	9.60 ± 3.14	8.80 ± 3.26
Liver, g	2.09 ± 0.23	2.16 ± 0.29	2.08 ± 0.29	2.21 ± 0.26	2.27 ± 0.44
Epididymal fat, g	1.00 ± 0.42	1.51 ± 0.80	0.97 ± 0.62	1.13 ± 0.48	1.15 ± 0.52
Kidney, g	0.51 ± 0.08[3]	0.59 ± 0.05	0.58 ± 0.63	0.55 ± 0.04	0.54 ± 0.05

[1] Values are means ± SD, $n = 10$. BW, body weight; Con, control mice fed AIN-93G diet and water; MGO, methylglyoxal or mice fed AIN-93G diet and 0.12% MGO in water; 0.1Q, mice fed 0.1% quercetin in diet plus 0.12% MGO in water; 0.2Q, mice fed 0.2% quercetin in diet plus 0.12% MGO in water; 0.4Q, mice fed 0.4% quercetin in diet plus 0.12% MGO in water.
[2] $P < 0.05$ compared with MGO.
[3] $P < 0.01$ compared with MGO.

°C. Then, ethyl acetate/tetrahydrofuran (10:1,800 μL) were added, sonicated (10 min), and centrifuged. The supernatant was aspirated. After the procedure was repeated 3 times, the combined supernatant was dried under nitrogen and reconstituted with 80% methanol (50 μL) for LC-MS/MS analysis after centrifugation at 16,000 × g for 15 min at 4 °C.

Preparation of feces, kidney, and liver samples.

One hundred milligrams of feces, kidney, and liver samples were homogenized with 1 mL PBS (pH 7.4, 1×) then sonicated for 30 min and centrifuged at 16,000 × g for 15 min at 4 °C. The homogenate (200 μL) was further processed following the same procedure for plasma and urine samples.

Determination and quantification of the MGO adducts of quercetin and its metabolites.

The MS^2 and MS^3 spectra of quercetin, isorhamnetin, and their MGO adducts were obtained using the LTQ Velos Pro ion trap mass spectrometer (Thermo Electron) equipped with an electrospray ionization (ESI) interface. The concentrations of quercetin, isorhamnetin, and their MGO adducts were quantified using a Thermo Q Exactive™ Plus Orbitrap™ mass spectrometer equipped with a heated ESI (HESI) and a Vanquish ultra-high pressure liquid chromatography (UHPLC) (Thermo Fisher Scientific). Detailed information is listed in the **Supplementary methods**.

Quercetin (30.2 mg) and isorhamnetin (31.5 mg) and MGO (45.5 μL, 40% in H_2O) were dissolved and mixed in 10.0 mL phosphate buffer (0.1 M, pH 7.4), respectively. The mixed solution was incubated at 37°C for 3 h and dried out by a stream of N_2. The residue was reconstituted into 50% methanol (500 μL) with 0.1% formic acid (FA) and centrifuged at 16000 × g for 10 min at 4 °C for LC-MS analysis. The extracted ions were used as in situ references for the identification of MGO conjugates of quercetin and isorhamnetin in mice. In addition, the concentrations of the MGO adducts of quercetin and isorhamnetin were expressed as quercetin and isorhamnetin equivalents, respectively.

Western blot assay of proteins

Kidney and liver tissues (100 mg each) were homogenized in RIPA buffer. The samples of tissue lysate were prepared for Western blot to determine the protein expressions of GLO I and II (1:500 dilution), AR (1:500 dilution), and β-actin (1:2000 dilution) as described previously (21, 29). The band intensity was analyzed by ImageJ software and the ratio to β-actin was presented by setting the value of the control as 1.

Statistical analysis

All values are presented as means ± SDs. One-way ANOVA with Dunnett's test was used to analyze the control and experimental groups compared with the MGO group using GraphPad 8.0.1 to determine the effects of MGO in normal mice and the effects of quercetin in MGO-administered mice **Table 1** and **Figures 1-3**. Also, 1-way ANOVA with Tukey test was employed to determine whether the plasma and liver concentrations of quercetin, isorhamnetin, and their respective MGO-trapping adducts responded to quercetin dose for **Figure 4** and **Table 2**. Data were tested using Levene's test to verify that variances were homogeneous. $P < 0.05$ was considered statistically significant.

Results

Effects of dietary quercetin on MGO-induced BW gain in MGO-administered mice

After 1 wk of MGO administration, the BW and organ weights of MGO mice did not significantly change compared with those of Con mice (data not shown). However, the mouse weight gain (by 51%) and kidney weight after 6 wk of MGO administration were significantly higher than those of Con mice ($P < 0.05$ and $P < 0.01$, respectively), but the liver and epididymal fat weights were not altered in MGO mice compared with Con mice (Table 1). The weight gain in 0.1Q was significantly less (by 31%, $P < 0.05$) than that in MGO mice, but not in 0.2Q (by 19.5%, $P = 0.31$) and 0.4Q (by 26.2%, $P = 0.11$). Also, the organ weights were not altered by the quercetin treatments compared with those in MGO mice (Table 1).

Effects of dietary quercetin on the concentrations of MGO and AGEs in MGO-administered mice

As shown in Figure 1A–C, the MGO concentrations in plasma (by 2.88-fold, $P < 0.001$), kidney (by 1.44-fold, $P < 0.05$), and liver (by 1.28-fold, $P < 0.05$) were significantly higher in MGO-treated mice after 1 wk of treatment than those in the Con group. Furthermore, the MGO concentrations in plasma (by 6-fold, $P < 0.001$), kidney (by 1.80-fold, $P < 0.001$), and liver (by 1.54-fold, $P < 0.001$) were significantly higher in MGO-treated mice after 6 wk of treatment than those in the Con mice (Figure 1D–F). Meanwhile, the concentrations of AGEs in kidney (by 1.61-fold, $P < 0.001$) and liver (by 1.51-fold, $P < 0.001$) were significantly higher in MGO-administered mice after 6 wk of treatment than those in the Con mice (Figure 1G and H).

After 1 wk of treatment, the MGO concentrations in plasma and kidney were significantly lower (by 20.2%, $P < 0.01$ and 29.9%, $P < 0.05$, respectively) in 0.2Q mice than those in the MGO mice. The liver MGO concentration was reduced by 15.4% in 0.2Q group, but the difference was not statistically significant due to the large variation in the MGO group (Figure 1C). Moreover, after the 6 wk of treatment, the plasma MGO concentrations were significantly lower in 0.1Q (by 14.7%, $P < 0.05$), 0.2Q (by 18.6%, $P < 0.01$), and 0.4Q (by 14.9%, $P < 0.01$) than those in MGO mice (Figure 1D). Also,

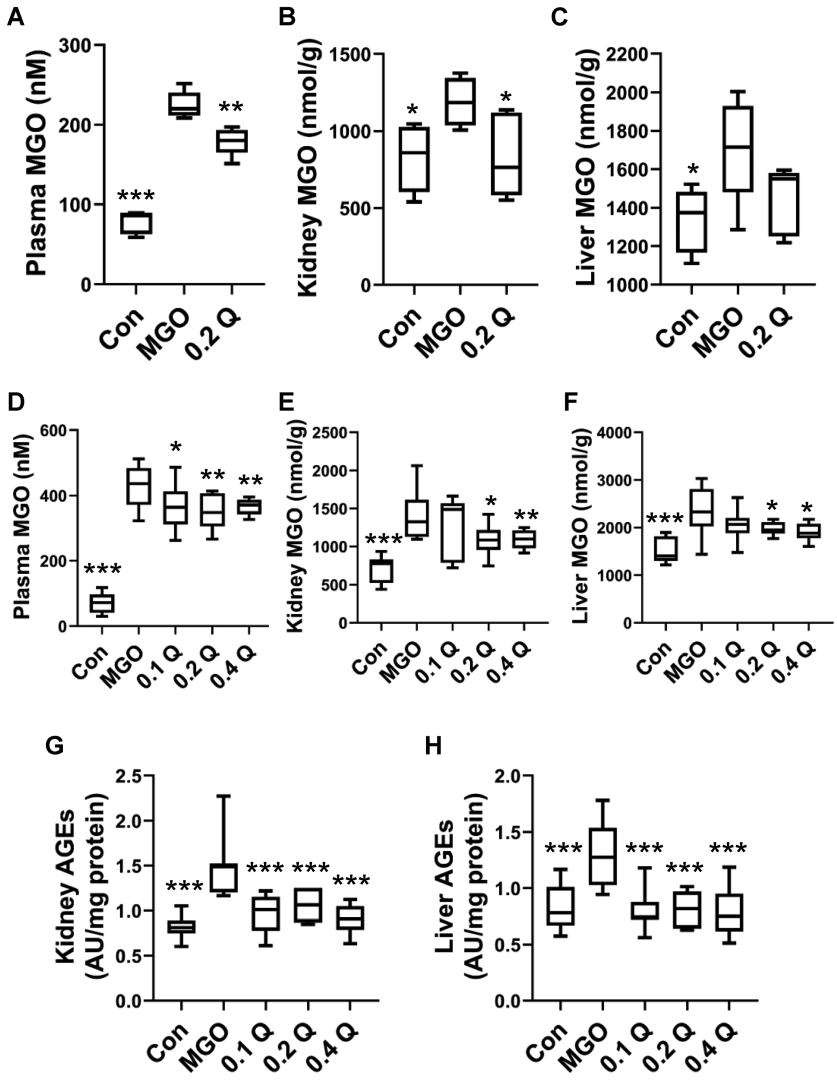

FIGURE 1 Dietary quercetin reduced the concentrations of MGO (A-C, 1 wk; D-F, 6 wk) and AGEs (G-H) in plasma, liver, and kidney of mice fed the control diet and water (Con) or 0.12% MGO in water (MGO), or 0.12% MGO in water and diet containing 0.2Q for 1 wk (experiment 1) and diet containing 0.1Q, 0.2Q, or 0.4Q for 6 wk (experiment 2). Values are presented as mean ± SD represented by vertical bars, $n = 5$ for A-C and $n = 10$ for D-H. Different from MGO group: $^{*}P < 0.05$, $^{**}P < 0.01$, $^{***}P < 0.001$. AGE, advanced glycation end product; AU, arbitrary units; Con, control mice fed AIN-93G diet and water; MGO, methylglyoxal; MGO group, MGO mice fed AIN-93G diet and 0.12% MGO in water; 0.1Q, mice fed 0.1% quercetin in diet plus 0.12% MGO in water; 0.2Q, mice fed 0.2% quercetin in diet plus 0.12% MGO in water; 0.4Q, mice fed 0.4% quercetin in diet plus 0.12% MGO in water.

the MGO concentrations in kidney and liver were significantly lower in 0.2Q (by 20.8% and 15.4%; $P < 0.05$ for both) and 0.4Q (by 20% and 18.6%, $P < 0.05$ and $P < 0.01$, respectively) than those in MGO mice (Figure 1E and F). Meanwhile, the concentrations of AGEs in kidney and liver were significantly lower in 0.1Q, 0.2Q, and 0.4Q mice (by 28–36% and 35.2–36.8%; $P < 0.001$ for both, respectively) than those in MGO mice (Figure 1G and H).

Dietary quercetin and its metabolite isorhamnetin dose-dependently trap MGO

The presence of quercetin and its methylated metabolite, isorhamnetin, in mouse urine, feces, plasma, liver, and kidney was confirmed using authentic standards based on the corresponding retention time and typical MS^2 and MS^3 data (**Supplementary Figure 1**). As shown in Supplementary Figure 1, there is a peak at 7.22 min in mouse urine samples responding to the search of the mono-MGO adduct of quercetin ($[M-H]^-$ at *m/z* 373), which had a fragment ion at *m/z* 301 that lost 1 MGO unit. The MS^3 spectrum of this fragment ion (*m/z* 301/373) is almost identical to the MS^2 spectrum of quercetin (data not shown), suggesting it is the mono-MGO adduct of quercetin. Moreover, this peak has the same retention time and fragment ions as those of the mono-MGO adduct synthesized from the in vitro reaction (Supplementary Figure 1). Similarly, the presence of mono-MGO adduct of isorhamnetin ($[M-H]^-$ at *m/z* 387) was confirmed by further analyzing its MS^2 and MS^3 spectra and comparing them with those of the mono-MGO isorhamnetin synthesized from the in vitro reaction (Supplementary Figure 1).

The concentrations of quercetin, isorhamnetin, and their mono-MGO adducts were quantified based on the standard curves of quercetin and isorhamnetin, respectively. As shown in Figure 4A and B, the concentrations of quercetin and isorhamnetin in plasma were dose-dependently increased by quercetin administration. Similarly, the concentration of plasma

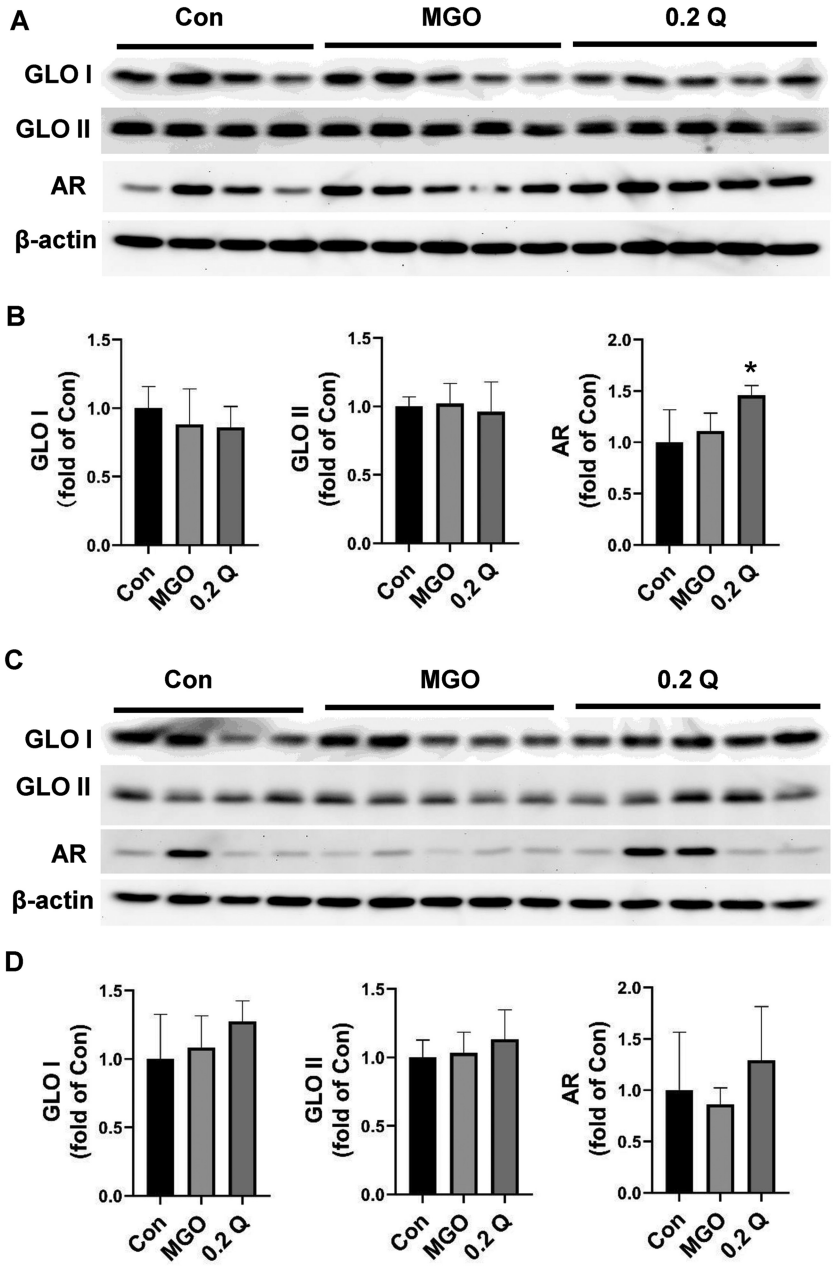

FIGURE 2 Protein expressions of GLO I and II, and AR in the kidney (A) and liver (B) of MGO-administered mice fed the control diet and water (Con) or 0.12% MGO in water (MGO), or 0.12% MGO in water and diet containing 0.2Q for 1 wk (experiment 1). Values are presented as mean ± SD represented by vertical bars, $n = 5$. Different from MGO group: $^*P < 0.05$. AR, aldose reductase; Con, control mice fed AIN-93G diet and water; GLO, glyoxalases; MGO, methylglyoxal; MGO group, MGO mice fed AIN-93G diet and 0.12% MGO in water; 0.2Q, mice fed 0.2% quercetin in diet plus 0.12% MGO in water.

mono-MGO conjugated quercetin in 0.4Q was significantly higher than those in 0.1Q mice ($P < 0.05$). However, there was no statistically significant difference between 0.2Q and 0.1Q and 0.2Q and 0.4Q (Figure 4C). Moreover, the mono-MGO–conjugated isorhamnetin in plasma was also dose-dependently increased by quercetin administration similarly to isorhamnetin concentrations (Figure 4D).

Furthermore, the concentrations of quercetin, isorhamnetin, and their MGO adducts in the samples of urine and feces were increased as the dose of quercetin increased from 0.1Q to 0.4Q (Table 2). Moreover, the concentrations of quercetin and isorhamnetin in the liver were not responsive to quercetin dose. The mono-MGO–conjugated quercetin was identified in liver and kidney samples of 0.1Q, 0.2Q, and 0.4Q mice but at very low concentrations. However, the MGO adduct of isorhamnetin was not detected in the liver and kidney samples (Table 2).

Dietary quercetin activates the detoxification enzymes of MGO

After 1 wk of treatment, MGO did not significantly change the expressions of GLO I and II, the main enzymes for MGO detoxification, and AR, another important MGO detoxification

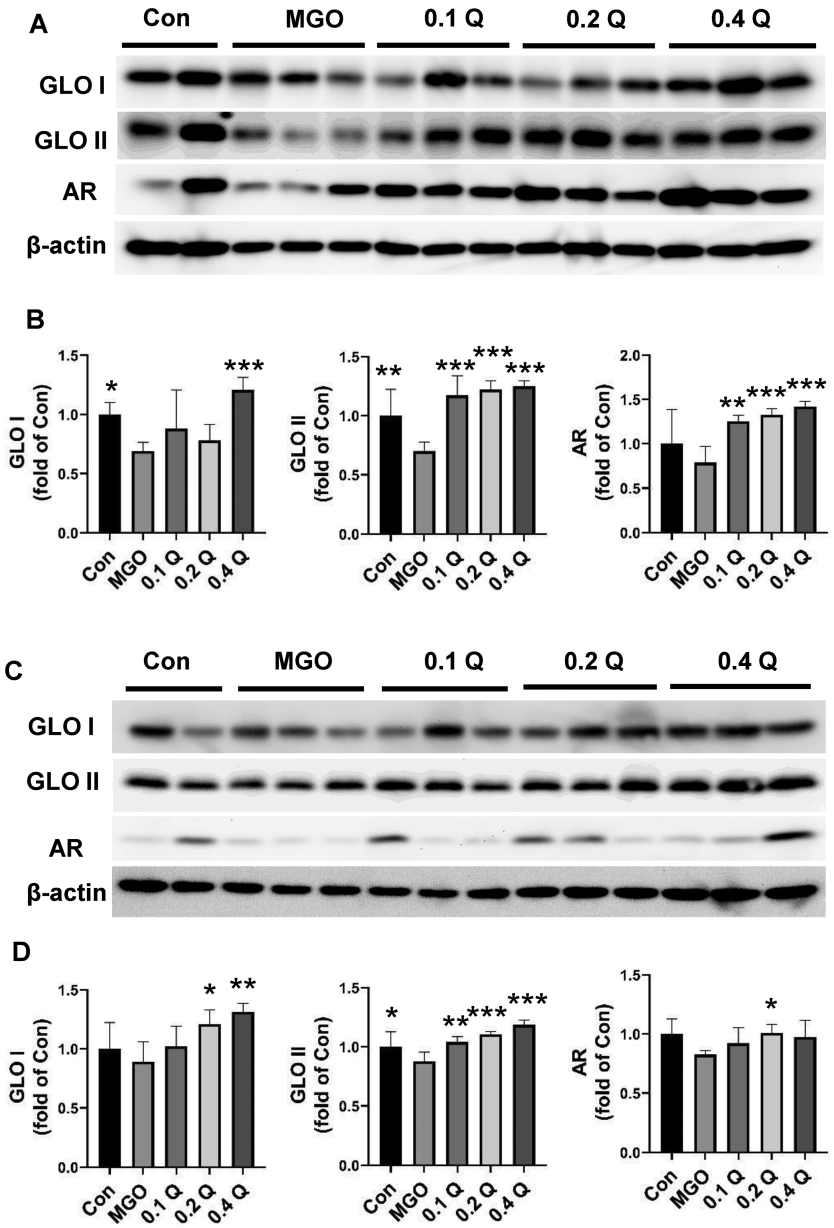

FIGURE 3 Protein expressions of GLO I and II, and AR in the kidney (A) and liver (B) of MGO-administered mice fed the control diet and water (Con) or 0.12% MGO in water (MGO), or 0.12% MGO in water and diet containing 0.1Q, 0.2Q, or 0.4Q for 6 wk (experiment 2). Values are presented as mean ± SD, $n = 10$. Different from MGO group: $^{*}P < 0.05$, $^{**}P < 0.01$, $^{***}P < 0.001$. AR, aldose reductase; Con, control mice fed AIN-93G diet and water; GLO, glyoxalases; MGO, methylglyoxal; MGO group, MGO mice fed AIN-93G diet and 0.12% MGO in water; 0.1Q, mice fed 0.1% quercetin in diet plus 0.12% MGO in water; 0.2Q, mice fed 0.2% quercetin in diet plus 0.12% MGO in water; 0.4Q, mice fed 0.4% quercetin in diet plus 0.12% MGO in water.

enzyme, in kidney and liver (Figure 2) compared with the Con group. The expressions of AR in 0.2Q mice were significantly upregulated by 31.2% in the kidney ($P < 0.05$, Figure 2A and B) but not the liver (Figure 2C and D), and the expressions of GLO I and GLO II in 0.2Q mice did not significantly change in the kidney and liver compared with those of MGO mice (Figure 2).

In kidney, the expressions of GLO I and GLO II were significantly higher in MGO mice after 6 wk of treatment (by 31%, $P < 0.05$ and 30%, $P < 0.01$, respectively) than those in Con mice. The GLO I expressions were significantly upregulated in 0.4Q mice (1.86-fold increase, $P < 0.001$) compared with MGO mice, but not in 0.1Q and 0.2Q mice (Figure 3A and B). All 3 quercetin doses significantly upregulated the expression of GLO II (1.67- to 1.78-fold change compared with the MGO group, $P < 0.001$) (Figure 3A and B). Moreover, the AR expression was significantly upregulated by 0.1Q (1.59-fold, $P < 0.01$), 0.2Q (1.68-fold, $P < 0.001$), and 0.4Q (1.80-fold, $P < 0.001$) after 6 wk of treatment compared with that in the MGO group (Figure 3A and B). In liver, the expressions of GLO I (1.36-fold in 0.2Q, $P < 0.01$; 1.48-fold in 0.4Q, $P < 0.001$) and GLO II (1.19-fold in 0.1Q, $P < 0.01$; 1.26-fold in 0.2Q, $P < 0.001$; 1.35-fold in 0.4Q, $P < 0.001$), and AR (1.22-fold in 0.2Q, $P < 0.05$) were significantly upregulated by quercetin treatments compared with those in the MGO mice (Figure 3C and D).

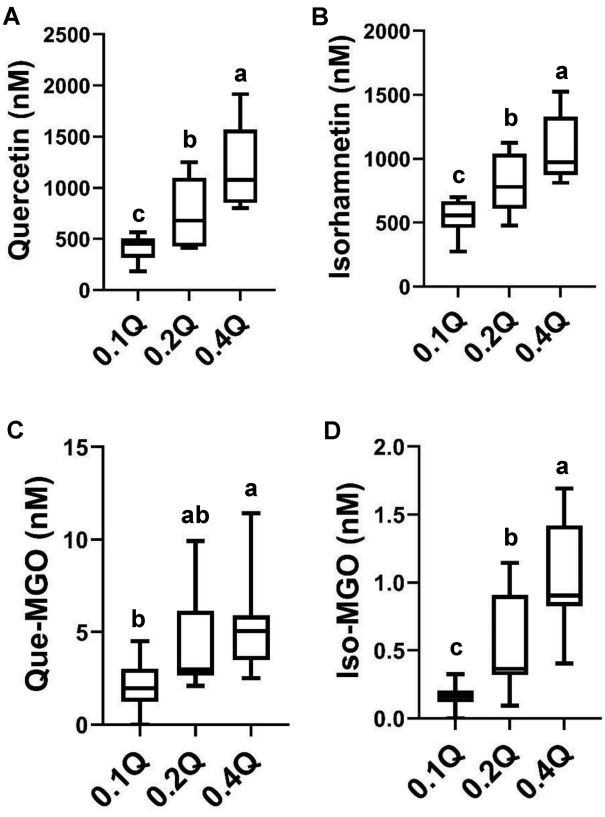

FIGURE 4 Plasma concentrations of quercetin (A), isorhamnetin (B), and their respective trapping adducts with MGO (C and D) in mice fed the control diet and water (Con) or 0.12% MGO in water (MGO), or 0.12% MGO in water and diet containing 0.1Q, 0.2Q, or 0.4Q for 6 wk (experiment 2). Values are presented as mean ± SD represented by vertical bars and analyzed by 1-way ANOVA with Tukey test, $n = 10$. Labeled means without a common letter differ, $P < 0.05$. MGO, methylglyoxal; Iso-MGO, trapping adduct of isorhamnetin with MGO; Que-MGO, trapping adduct of quercetin with MGO; 0.1Q, mice fed 0.1% quercetin in diet plus 0.12% MGO in water; 0.2Q, mice fed 0.2% quercetin in diet plus 0.12% MGO in water; 0.4Q, mice fed 0.4% quercetin in diet plus 0.12% MGO in water.

Discussion

MGO, a strong AGE precursor and a highly reactive dicarbonyl compound, can easily bind to and modify arginine, lysine, and cysteine residues to contribute to the formation of AGEs. The roles of AGEs in the pathogenesis of a number of chronic diseases have been well documented (2–8). Therefore, targeting MGO can be an effective approach to prevent or treat MGO and AGEs associated chronic diseases. In the current study, we found that dietary quercetin reduced the concentrations of MGO and inhibited the accumulation of AGEs in healthy mice treated with exogenous MGO. Further mechanistic investigations demonstrated that the decreased effects of quercetin on MGO and AGEs were related to 2 different pathways, the direct trapping of MGO by quercetin and its metabolite, isorhamnetin, to form the corresponding adducts, and the activation of MGO detoxification pathways of glyoxalase system and AR.

Many food products and beverages are exogenous sources of MGO (14, 15, 31). The administration of exogenous MGO has been used in animal models to investigate the impact of dietary MGO on AGE-associated diseases (2–8). In the previous studies, the MGO was given to the mice or rats at different doses by drinking water, oral gavage, and minipump subcutaneously for 4 wk and up to 5 mo. Compared to previous studies, the present study used a human-relevant dose, 0.12% MGO in drinking water (21), on healthy mice. This is the first study to demonstrated that 1 wk of MGO administration significantly increased plasma MGO concentrations compared with the those in control mice, and 6 wk of MGO treatment further increased the plasma MGO concentration (429 nM), which was 1.90 times higher than the plasma MGO concentration after 1 wk (225 nM) of MGO administration. These results indicate an accumulative effect of MGO administration on the elevation of MGO concentration in the circulatory system. Furthermore, significant accumulations of AGEs in tissues were observed after 6 wk but not after 1 wk of MGO administration, suggesting 1 wk of MGO treatment is not long enough to cause significant formations of AGEs. Results from the current study are consistent with previous studies in MGO-treated mice or rats. In mice, the plasma MGO concentrations were significantly increased in the apoE knockout and receptor of AGEs (RAGE)/apoE double-knockout mice given 1% MGO in drinking water for 6 wk (20) and in the combination of high-fat diet (HFD) and MGO-fed mice compared with the HFD-fed mice for 17 wk (21). In rats, after 3 mo of administration by gradually enhanced doses of MGO in drinking water from 50 mg/kg to 75 mg/kg in normal male rats, the plasma MGO was significantly increased to 590 nM at the same concentrations of aged rats (570 nM), compared with it in the control rats (280 nM) and diabetic rats that were not administered MGO (370 nM) (16, 17). Meanwhile, the increased AGE concentrations were also found after the MGO administration in rats (16, 17, 32). In other studies, it was observed that the addition of MGO to drinking water at different doses (1% for 4 wk, 50 mg/kg for 5 mo, and 75 mg/kg for 8 wk) elevated AGE concentrations (the plasma MGO concentration was not mentioned) (33–36). In rats MGO-administered by oral gavage at 600 mg/kg for 4 wk, the plasma MGO and AGEs were significantly increased (37). Similarly, the MGO concentrations in plasma and tissues were significantly elevated in rats after MGO administration at 60 mg/kg/d by minipump subcutaneously for 4 wk (19). The elevated MGO and AGEs concentrations observed in MGO-administered rodents were consistent with and mimicked the higher concentrations of MGO and AGEs in humans with diabetes and other diseases (38–42). Taken together, the MGO-administered rodents may be a suitable model to investigate the role of high concentrations of MGO and AGEs in the pathogenesis of related diseases.

It has been reported that quercetin, 1 of the major dietary flavonoids, possessed strong scavenging effects on MGO and inhibited AGE formation in vitro (22, 23, 43, 44). However, the efficacy of quercetin in vivo on lowering MGO and AGEs has not been widely studied. Only 1 human study was reported, in which quercetin 3-glucoside supplementation at 160 mg/d for 4 wk decreased plasma MGO concentrations without changing AGEs concentrations in apparently healthy (pre)hypertensive men and women (25). In the present mouse study, quercetin supplementation significantly reduced the concentrations of MGO and AGEs in mice after 6 wk of treatment at different doses of 0.1%, 0.2%, and 0.4%, which are consistent with the reported lowering MGO effects in humans and inhibiting AGE formation in vitro. The dose range of quercetin administration in mice is equivalent to 7.56–30 mg/kg in humans based on the practice guide of dose conversion from mice to humans (45). Considering the recommended dose from 250 to 1200 mg/d

TABLE 2 Concentrations of quercetin, isorhamnetin, and their respective trapping adducts with MGO in urine, feces, liver, and kidney samples of mice fed 0.12% MGO in water and diet containing 0.1Q, 0.2Q, or 0.4Q for 6 wk (experiment 2)[1]

Group	Quercetin[2]	Quercetin-MGO[3]	Isorhamnetin[4]	Iso-MGO[5]
Urine,[6] nmol/L				
0.1 Q	4210	42.3	1820	27.0
0.2 Q	6400	149	3050	40.4
0.4 Q	13100	238	4770	57.9
Feces,[6] nmol/g				
0.1 Q	23.4	0.38	2.05	0.0209
0.2 Q	28.0	1.60	2.89	0.0153
0.4 Q	45.0	1.67	3.95	0.0331
Liver,[7] nmol/g				
0.1 Q	8.60 ± 4.61	+	13.3 ± 6.68	—
0.2 Q	11.0 ± 8.00	+	21.4 ± 10.9	—
0.4 Q	9.18 ± 1.84	+	20.6 ± 3.99	—
Kidney, nmol/g				
0.1 Q	+	+	+	—
0.2 Q	+	+	+	—
0.4 Q	+	+	+	—

[1]Values are means ± SD, $n = 10$. Iso-MGO, isorhamnetin MGO adduct; MGO, methylglyoxal; +, detected, but cannot be quantified; —, not detected. 0.1Q, mice fed 0.1% quercetin in diet plus 0.12% MGO in water; 0.2Q, mice fed 0.2% quercetin in diet plus 0.12% MGO in water; 0.4Q, mice fed 0.4% quercetin in diet plus 0.12% MGO in water.
[2]Limit of detection (LOD) of quercetin: 0.13 nM in urine; 0.15 nM in feces/liver/kidney.
[3]The concentrations of the MGO adduct of quercetin were expressed as quercetin equivalents.
[4]LOD of isorhamnetin: 0.08 nM in urine; 0.09 nM in feces/liver/kidney.
[5]The concentrations of the MGO adduct of isorhamnetin were expressed as isorhamnetin equivalents.
[6]The pooled fecal and urine samples of 24 h were harvested from 1 cage of 5 mice in each group using the metabolic cage. Therefore, there is no SE for these data.
[7]The data were analyzed by 1-way ANOVA with Tukey's test and no statistical difference was observed.

of the commercial quercetin supplements and the reported quercetin supplementation of 1000 mg/d for 12 wk (27), the current equivalent doses of quercetin can be achievable and safe in humans.

This study demonstrated, to our knowledge for the first time, that quercetin has the capacity to trap MGO to form the MGO adduct in vivo and also showed a dose-dependent effect of trapping MGO. Furthermore, isorhamnetin, the methylated metabolite of quercetin, has the same A-ring as quercetin, which is the active site for the conjugation of MGO. Therefore, isorhamnetin was expected to trap MGO following the same mechanism as reported for quercetin (24), which was supported by the observation of the dose-dependent formation of the MGO adduct of isorhamnetin after 6 wk of quercetin treatment. Altogether, the mechanism, by directly trapping MGO using quercetin and isorhamnetin, contributed to lowering the MGO concentrations in the body.

Moreover, dietary quercetin activated the MGO detoxification systems of GLO and AR in kidney and liver tissues. Especially after the 6 wk of quercetin supplementation (experiment 2), the expressions of GLO I/II and AR were significantly upregulated in kidney and liver compared with those in MGO-treated mice. However, after the 1 wk of quercetin treatment (experiment 1), no significant change in the enzyme expressions was found in the kidney and liver, except for AR in the kidney. Similarly, it has been reported that quercetin decreased the AGEs concentrations and RAGE expression and increased the GLO I activity and expression in brains of diabetic rats (46). Therefore, it indicated that the activations of MGO detoxification enzymes by quercetin also contributed to lower the MGO concentrations in vivo.

In conclusion, the present study demonstrated that dietary quercetin significantly decreased the accumulation of MGO and AGEs in exogenous MGO–administered mice via trapping MGO directly and activating MGO detoxification pathways to indirectly lower the MGO concentrations in healthy mice. Considering the beneficial effects of scavenging MGO and inhibiting protein glycation and the abundant existence in fruits and vegetables, quercetin may be a promising dietary agent to potentially prevent and treat the diseases in which MGO and AGEs play a pivotal role.

Acknowledgments

The authors' responsibilities were as follows—SS, YZ: designed the research; YZ, YT: conducted the research and analyzed the data; SS, YZ, YT: wrote the manuscript; SS: had primary responsibility for the final content; and all authors: read and approved the final manuscript.

Reference

1. Singh R, Barden A, Mori T, Beilin L. Advanced glycation end-products: a review. Diabetologia 2001;44(2):129–46.
2. Sato T, Iwaki M, Shimogaito N, Wu X, Yamagishi S, Takeuchi M. TAGE (toxic AGEs) theory in diabetic complications. Curr Mol Med 2006;6(3):351–8.
3. Vlassara H, Uribarri J. Advanced glycation end products (AGE) and diabetes: cause, effect, or both? Curr Diab Rep 2014;14(1):453.
4. Vlassara H. Advanced glycation end-products and atherosclerosis. Ann Med 1996;28(5):419–26.
5. Gaens KH, Stehouwer CD, Schalkwijk CG. Advanced glycation endproducts and its receptor for advanced glycation endproducts in obesity. Curr Opin Lipidol 2013;24(1):4–11.

6. Thornalley PJ. Advanced glycation end products in renal failure. J Ren Nutr 2006;16(3):178–84.
7. Luevano-Contreras C, Chapman-Novakofski K. Dietary advanced glycation end products and aging. Nutrients 2010;2(12):1247–65.
8. Srikanth V, Maczurek A, Phan T, Steele M, Westcott B, Juskiw D, Munch G. Advanced glycation endproducts and their receptor RAGE in Alzheimer's disease. Neurobiol Aging 2011;32(5):763–77.
9. Chakraborty S, Karmakar K, Chakravortty D. Cells producing their own nemesis: understanding methylglyoxal metabolism. IUBMB Life 2014;66(10):667–78.
10. Kalapos MP. The tandem of free radicals and methylglyoxal. Chem Biol Interact 2008;171(3):251–71.
11. Rabbani N, Thornalley PJ. Methylglyoxal, glyoxalase 1 and the dicarbonyl proteome. Amino Acids 2012;42(4):1133–42.
12. Vistoli G, De Maddis D, Cipak A, Zarkovic N, Carini M, Aldini G. Advanced glycoxidation and lipoxidation end products (AGEs and ALEs): an overview of their mechanisms of formation. Free Radic Res 2013;47(sup1):3–27.
13. Matafome P, Sena C, Seica R. Methylglyoxal, obesity, and diabetes. Endocrine 2013;43(3):472–84.
14. Tan D, Wang Y, Lo CY, Ho CT. Methylglyoxal: its presence and potential scavengers. Asia Pac J Clin Nutr 2008;17(Suppl 1):261–4.
15. Nemet I, Varga-Defterdarović L, Turk Z. Methylglyoxal in food and living organisms. Mol Nutr Food Res 2006;50(12):1105–17.
16. Crisostomo J, Matafome P, Santos-Silva D, Rodrigues L, Sena CM, Pereira P, Seica R. Methylglyoxal chronic administration promotes diabetes-like cardiac ischaemia disease in Wistar normal rats. Nutr Metab Cardiovasc Dis 2013;23(12):1223–30.
17. Rodrigues L, Matafome P, Crisóstomo J, Santos-Silva D, Sena C, Pereira P, Seiça R. Advanced glycation end products and diabetic nephropathy: a comparative study using diabetic and normal rats with methylglyoxal-induced glycation. J Physiol Biochem 2014;70(1):173–84.
18. Lee B-H, Hsu W-H, Chang Y-Y, Kuo H-F, Hsu Y-W, Pan T-M. Ankaflavin: a natural novel PPARγ agonist upregulates Nrf2 to attenuate methylglyoxal-induced diabetes in vivo. Free Radic Biol Med 2012;53(11):2008–16.
19. Dhar A, Dhar I, Jiang B, Desai KM, Wu L. Chronic methylglyoxal infusion by minipump causes pancreatic β-cell dysfunction and induces type 2 diabetes in Sprague-Dawley rats. Diabetes 2011;60(3):899–908.
20. Tikellis C, Pickering RJ, Tsorotes D, Huet O, Cooper ME, Jandeleit-Dahm K, MC T. Dicarbonyl stress in the absence of hyperglycemia increases endothelial inflammation and atherogenesis similar to that observed in diabetes. Diabetes 2014;63(11):3915–25.
21. Zhao Y, Wang P, Sang S. Dietary genistein inhibits methylglyoxal-induced advanced glycation end product formation in mice fed a high-fat diet. J Nutr 2019;149(5):776–87.
22. Li X, Zheng T, Sang S, Lv L. Quercetin inhibits advanced glycation end product formation by trapping methylglyoxal and glyoxal. J Agric Food Chem 2014;62(50):12152–8.
23. Bhuiyan MN, Mitsuhashi S, Sigetomi K, Ubukata M. Quercetin inhibits advanced glycation end product formation via chelating metal ions, trapping methylglyoxal, and trapping reactive oxygen species. Biosci Biotechnol Biochem 2017;81(5):882–90.
24. Liu G, Xia Q, Lu Y, Zheng T, Sang S, Lv L. Influence of quercetin and its methylglyoxal adducts on the formation of α-dicarbonyl compounds in a lysine/glucose model system. J Agric Food Chem 2017;65(10):2233–9.
25. Van den Eynde MDG, Geleijnse JM, Scheijen J, Hanssen NMJ, Dower JI, Afman LA, Stehouwer CDA, Hollman PCH, Schalkwijk CG. Quercetin, but not epicatechin, decreases plasma concentrations of methylglyoxal in adults in a randomized, double-blind, placebo-controlled, crossover trial with pure flavonoids. J Nutr 2018;148(12):1911–6.
26. . In: Olson E, Graham D. Padmanabhan S. Chapter 5 - animal models in pharmacogenomics, ed. Handbook of pharmacogenomics and stratified medicine. San Diego: Academic Press; 2014. p. 73–87.
27. Jin F, Nieman DC, Shanely RA, Knab AM, Austin MD, Sha W. The variable plasma quercetin response to 12-week quercetin supplementation in humans. Eur J Clin Nutr 2010;64(7):692–7.
28. Tang Y, Zhao Y, Wang P, Sang S. Simultaneous determination of multiple reactive carbonyl species in high fat diet-induced metabolic disordered mice and the inhibitory effects of rosemary on carbonyl stress. J Agric Food Chem 69, 3,1123–31, 2021 DOI:10.1021/acs.jafc.0c07748.
29. Zhao Y, Zhu Y, Wang P, Sang S. Dietary genistein reduces methylglyoxal and advanced glycation end product accumulation in obese mice treated with high-fat diet. J Agric Food Chem 2020;68(28):7416–24.
30. Zhao Y, Sedighi R, Wang P, Chen H, Zhu Y, Sang S. Carnosic acid as a major bioactive component in rosemary extract ameliorates high-fat-diet-induced obesity and metabolic syndrome in mice. J Agric Food Chem 2015;63(19):4843–52.
31. Degen J, Hellwig M, Henle T. 1,2-dicarbonyl compounds in commonly consumed foods. J Agric Food Chem 2012;60(28):7071–9.
32. Sena CM, Matafome P, Crisostomo J, Rodrigues L, Fernandes R, Pereira P, Seica RM. Methylglyoxal promotes oxidative stress and endothelial dysfunction. Pharmacol Res 2012;65(5):497–506.
33. Guo Q, Mori T, Jiang Y, Hu C, Osaki Y, Yoneki Y, Sun Y, Hosoya T, Kawamata A, Ogawa S, et al. Methylglyoxal contributes to the development of insulin resistance and salt sensitivity in Sprague-Dawley rats. J Hypertens 2009;27(8):1664–71.
34. Golej J, Hoeger H, Radner W, Unfried G, Lubec G. Oral administration of methylglyoxal leads to kidney collagen accumulation in the mouse. Life Sci 1998;63(9):801–7.
35. Rodrigues T, Matafome P, Seiça R. Methylglyoxal further impairs adipose tissue metabolism after partial decrease of blood supply. Arch Physiol Biochem 2013;119(5):209–18.
36. Rodrigues T, Matafome P, Santos-Silva D, Sena C, Seica R. Reduction of methylglyoxal-induced glycation by pyridoxamine improves adipose tissue microvascular lesions. J Diabetes Res 2013;2013:1.
37. Hsu WH, Lee BH, Chang YY, Hsu YW, Pan TM. A novel natural Nrf2 activator with PPARγ-agonist (monascin) attenuates the toxicity of methylglyoxal and hyperglycemia. Toxicol Appl Pharmacol 2013;272(3):842–51.
38. Beisswenger PJ, Howell SK, Russell GB, Miller ME, Rich SS, Mauer M. Early progression of diabetic nephropathy correlates with methylglyoxal-derived advanced glycation end products. Diabetes Care 2013;36(10):3234.
39. Hanssen NMJ, Scheijen J, Jorsal A, Parving H-H, Tarnow L, Rossing P, Stehouwer CDA, Schalkwijk CG. Higher plasma methylglyoxal levels are associated with incident cardiovascular disease in individuals with type 1 diabetes: a 12-year follow-up study. Diabetes 2017;66(8):2278.
40. Kong X, Ma MZ, Huang K, Qin L, Zhang HM, Yang Z, Li XY, Su Q. Increased plasma levels of the methylglyoxal in patients with newly diagnosed type 2 diabetes 2. J Diabetes 2014;6(6):535–40.
41. Han Y, Randell E, Vasdev S, Gill V, Gadag V, Newhook LA, Grant M, Hagerty D. Plasma methylglyoxal and glyoxal are elevated and related to early membrane alteration in young, complication-free patients with type 1 diabetes. Mol Cell Biochem 2007;305(1-2):123–31.
42. Masania J, Malczewska-Malec M, Razny U, Goralska J, Zdzienicka A, Kiec-Wilk B, Gruca A, Stancel-Mozwillo J, Dembinska-Kiec A, Rabbani N, et al. Dicarbonyl stress in clinical obesity. Glycoconj J 2016;33(4):581–9.
43. Alam MM, Ahmad I, Naseem I. Inhibitory effect of quercetin in the formation of advance glycation end products of human serum albumin: an in vitro and molecular interaction study. Int J Biol Macromol 2015;79:336–43.
44. Ashraf JM, Shahab U, Tabrez S, Lee EJ, Choi I, Ahmad S. Quercetin as a finer substitute to aminoguanidine in the inhibition of glycation products. Int J Biol Macromol 2015;77:188–92.
45. Nair AB, Jacob S. A simple practice guide for dose conversion between animals and human. J Basic Clin Pharm 2016;7(2):27–31.
46. Zhu X, Cheng YQ, Lu Q, Du L, Yin XX, Liu YW. Enhancement of glyoxalase 1, a polyfunctional defense enzyme, by quercetin in the brain in streptozotocin-induced diabetic rats. Naunyn-Schmiedeberg's Arch Pharmacol 2018;391(11):1237–45.